

## High-Resolution Alpha-Autoradiography with Contact Microscopy Technique

Kuniaki AMEMIYA<sup>1,\*</sup>, Hiroyuki TAKAHASHI<sup>2</sup>, Toru NARUSE<sup>1</sup>, Masaharu NAKAZAWA<sup>1</sup>,  
Yoshinobu NAKAGAWA<sup>3</sup>, Toshikazu MAJIMA<sup>4</sup>, Teruyoshi KAGEJI<sup>5</sup>,  
Yoshinori SAKURAI<sup>6</sup>, Tooru KOBAYASHI<sup>6</sup>, Nakahiro YASUDA<sup>7</sup>, Mikio YAMAMOTO<sup>7</sup>, Koichi OGURA<sup>8</sup>

<sup>1</sup>Department of Quantum Engineering and Systems Science, The University of Tokyo, Tokyo 113-8656, Japan

<sup>2</sup>Research into Artifacts, Center for Engineering, The University of Tokyo, Tokyo 153-8904, Japan

<sup>3</sup>Department of Neurosurgery, National Kagawa Children's Hospital, Kagawa 765-8501, Japan

<sup>4</sup>Photonics Research Institute, National Institute of Advanced Industrial Science and Technology, Ibaraki 305-8568, Japan

<sup>5</sup>Department of Neurological Surgery, The University of Tokushima, Tokushima 770-8503, Japan

<sup>6</sup>Research Reactor Institute, Kyoto University, Osaka 590-0494, Japan

<sup>7</sup>Research Center for Radiation Safety, National Institute of Radiological Sciences, Chiba 263-8555, Japan

<sup>8</sup>College of Industrial Technology, Nihon University, Chiba 275-8575, Japan

We have been developing a novel method for high-resolution neutron-induced alpha-autoradiography (NIAR) using CR-39 plastic track detectors and an atomic force microscope (AFM) with contact microscopy technique. In this technique, sliced samples such as tissues including boron compounds are mounted on CR-39 plates, and then irradiated by thermal neutrons. The irradiated samples are exposed to soft X-rays, and then etched in NaOH solution for short time. Etch pits for alpha/lithium particle tracks and relief for transmission X-ray image of the specimen can be observed on the CR-39 surface with an AFM at about 100 nm resolution. In the NIAR, discrimination of proton background is required for quantification of boron concentration, and incident angle measurement is significant for accurate positioning of the alpha/lithium tracks on the specimen image. These properties were tested for the measurement of small etch pits observed with an AFM. It was confirmed that alpha/lithium particles and protons could be distinguished by etch pit size, and that incident angle of those charged particles could be measured at the accuracy of several degrees. These informations approve the reliability of the NIAR, especially for the subcellular measurement of boron compound distribution inside a cell in boron neutron capture therapy (BNCT).

**KEYWORDS:** CR-39, solid state nuclear track detector, atomic force microscope, X-ray microscopy, alpha-autoradiography, boron neutron capture therapy

### I. Introduction

Autoradiography technique has been used for the measurements of specific compounds delivery in biological tissues or cells by labeling the compounds with radioisotopes. In alpha-autoradiography, alpha emitting isotopes are labeled and the emitted alpha particles are detected by imaging detectors such as photo films, solid state track detectors, imaging plates, and so on. In particular, neutron-induced alpha-autoradiography<sup>1,2)</sup> (NIAR) enables us to measure the distribution of the compounds labeled with boron by detecting alpha particles from  $^{10}\text{B}(n,\alpha)^7\text{Li}$  reactions without injuring the biological specimen by radiation during compound delivery.

NIAR has been used for the measurement of boron compound distribution in boron neutron capture therapy<sup>3)</sup> (BNCT). BNCT is a promising radiotherapy to kill malignant tumor cells selectively using short-range ( $\sim$  single cell size: 10  $\mu\text{m}$ ) charged particles from boron neutron reactions. It is significant in the therapy whether the boron-delivering compounds are distributed only in tumor tissues and whether the emitted alpha/lithium particles bring enough damage to break strand of DNA in tumor cells. Therefore there are demands for investigating boron compound distribution inside a cell in the therapy. For this purpose, the NIAR technique has been used for the measurement of boron compound distribution. How-

ever, it is quite difficult to measure boron distribution at sub-cellular scale using conventional autoradiography techniques with optical microscope observation.

Recently we have developed a new high-resolution alpha-autoradiography technique for the measurement of boron compound distribution using CR-39 plastic track detectors with atomic force microscope (AFM) readout. In this technique, we can detect the incident position of alpha/lithium particles at resolution of several tens of nanometer<sup>4)</sup> in histological image of biological cells with contact X-ray microscopy<sup>5,6)</sup> using CR-39 plastics.<sup>7)</sup> The imaging resolution is  $< 100$  nm, therefore we can visualize the local rate of boron neutron reactions inside cells at an intracellular structure level.

In the technique, however, we should note that there are still some points to be discussed: first, there are inevitable background protons in NIAR due to  $^{14}\text{N}(n,p)^{14}\text{C}$  reactions and recoils by fast neutrons. Although those components should be considered for microdosimetry in BNCT, we must eliminate them from the counts for the measurement of boron compound distribution. Second, the alpha/lithium particles are emitted almost isotropically, so that alpha/lithium particles with large incident angle degrade the accuracy of positioning the sources of those particles. In optical microscopy observation, those components can be eliminated: Alpha/lithium particles and protons can be discriminated by the size of etch pits.<sup>8)</sup> Incident angle of charged particles can be derived from the elliptical shape of the opening mouth of etch pits. In

\* Corresponding author, Tel. +81-3-5841-6974, Fax. +81-3-3818-3455, E-mail: kuni@sophie.q.t.u-tokyo.ac.jp

this paper, we describe that we can eliminate those disturbing components even with AFM readout using CR-39 plastics.

## II. Materials and Methods

### 1. Alpha particle mapping on cellular image

Experimental procedures for visualizing boron compound distribution inside tumor cells are described schematically in Fig. 1. The procedures mainly consist of following three parts: (1) detection of alpha/lithium particles through boron-neutron reactions using CR-39 plastic track detectors, (2) recording transmission X-ray image of tumor cells on the CR-39 plastics, (3) observation of the CR-39 surface with an atomic force microscope after etching process.

With an AFM, it is possible to observe alpha tracks as small etch pits of 80 nm in diameter on CR-39<sup>4)</sup> and relief of transmission soft X-ray image on the CR-39 can be also visualized at the resolution of better than 100 nm.<sup>7)</sup> Therefore we can achieve subcellular mapping of alpha/lithium tracks in X-ray image of detailed cell structure as relief on CR-39 plastics with AFM readout.

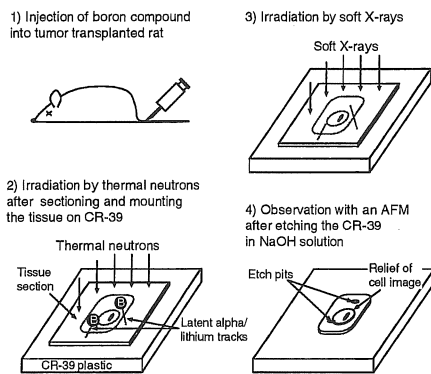


Fig. 1 The schematic flow of the high-resolution alpha-autoradiography for boron imaging inside tumor cells.

### 2. Discrimination between alpha/lithium particles and proton background

In the neutron induced alpha-autoradiography, we should discriminate the counts of alpha/lithium tracks from that of background protons for boron imaging in BNCT. Fortunately, CR-39 plates have the resolution for linear energy transfer (LET). The track sensitivity (size) of etch pits increases as the LET value of incident particles increases. Figure 2 shows the LET value of alpha/lithium particles and protons in water. The LET for protons is less than about 100 keV/ $\mu\text{m}$  and that for the alpha/lithium particles is ranged up to 250 – 350 keV/ $\mu\text{m}$  by calculation with TRIM code. Therefore, eliminating the counts for the particles having the LET value of less than 100 keV/ $\mu\text{m}$  will enable us to eliminate background protons.

We have tested the discrimination between alpha/lithium particles and background protons with the size of etch pits. CR-39 plates named BARYOTRAK from Fukuvi Chemical Industry, Japan was used in the present experiments. The

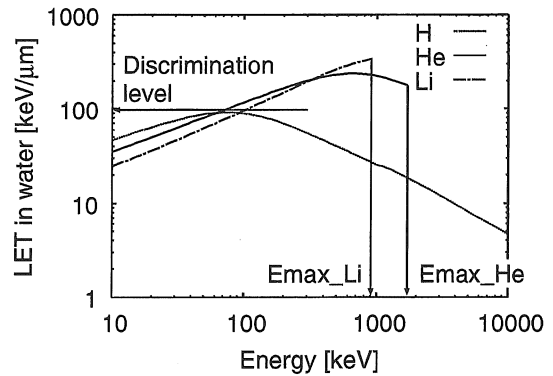


Fig. 2 Relation between LET value and energy of incident charged particle.

CR-39 plates were cut into 1 cm x 1 cm. The CR-39 pieces were mounted on the sample holder in a vacuum chamber ( $10^{-6}$  torr) and irradiated by protons of 200 keV, 500 keV, 700 keV and 1 MeV or alpha particles of 700 keV, 1 MeV, 1.47 MeV and 3 MeV from a Tandemron accelerator RAPID of RCNST, The University of Tokyo. The fluence of irradiated particles was  $5 \times 10^8 / \text{cm}^2$ . The CR-39 samples were taken out from the vacuum chamber within 2 hours after mounting on the sample holder to avoid vacuum effect to the track sensitivity of CR-39.<sup>9)</sup> The irradiated CR-39 pieces were etched in 7 N NaOH solution at 70 °C for 5 min. The surface of the etched CR-39 pieces was scanned with an AFM

We have also tested the particle identification with a CR-39 plastic irradiated by 1 MeV alpha particles of  $5 \times 10^8 / \text{cm}^2$  through 3.7  $\mu\text{m}$  thick Ni mesh having 17  $\mu\text{m}$  grid, and 200 keV protons ( $\sim 70$  keV/ $\mu\text{m}$ ) of  $10^8 / \text{cm}^2$ . The irradiated CR-39 was etched in the NaOH solution mentioned above for 2 min, and then the CR-39 surface was observed with the AFM.

### 3. Incident angle measurement

When charged particles impact with certain incident angle, the mouth shape of etch pits for those particles would be ellipse (see Fig. 3). We can calculate the incident angle from the mouth shape (major and minor axes of the ellipse,  $D$ ,  $d$ ) and the amount of bulk etch  $B$  as following formula,

$$\theta = \cos^{-1} \left( \frac{4B^2 + d^2}{\sqrt{16D^2B^2 + (4B^2 - d^2)^2}} \right). \quad (1)$$

Using the above formula, however, the derived incident angle has very large uncertainty when charged particles incident near normally. On the other hand, we can observe the three dimensional shape of the etch pits with the AFM, so that the incident angle can be estimated from the half cone angle  $\delta$  and most gentle gradient angle of the cone wall  $\phi$  as  $\theta = \delta + \phi$  (Fig. 3 (b)). When charged particles impact with large incident angle, however, the etch pit cones recline very much. Consequently the tip of the AFM cannot reach the tips of the etch pit cones. In that case we calculated the half cone angle

from the track sensitivity  $S$  of those etch pits with the following formula,

$$\delta = \sin^{-1} \left( \frac{1}{1+S} \right). \quad (2)$$

Where  $S$  can be derived from the mouth shape of the etch pits and bulk etch as follows,

$$S = \sqrt{\frac{16D^2B^2}{(4B^2 - d^2)^2} + 1} - 1. \quad (3)$$

In order to test the incident angle measurements of charged particles with CR-39 plastics and AFM readout, CR-39 pieces were irradiated by 500 MeV/n Fe ions of  $10^8/\text{cm}^2$  available from heavy ion medical accelerator in Chiba (HIMAC), National Institute of Radiological Sciences, Japan, with the incident angles of  $90^\circ$ ,  $75^\circ$ ,  $60^\circ$ ,  $45^\circ$  and  $30^\circ$ . The LET value of 500 MeV/n Fe ions is  $\sim 180 \text{ keV}/\mu\text{m}$  in water, which is comparable to that of MeV order alpha particles. High-energy heavy ions such as those Fe ions can penetrate the CR-39 plate ( $= 1 \text{ mm}$  thick), so that the incident angle can be also derived from the position difference between the etch pit on the surface and that on the backside under optical microscopic observation (Fig. 3(c)). Using this method, the incident angle can be calculated with the accuracy of  $0.1^\circ$ , therefore we used this method to measure the accurate nominal incident angle of charged particles with less irradiated CR-39 pieces of  $10^3/\text{cm}^2$  in fluence. The irradiated samples were etched in 7M NaOH solution at  $70^\circ\text{C}$  for 10 min, and observed with the AFM.

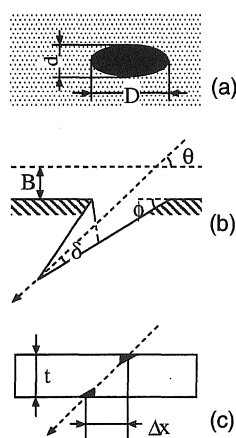


Fig. 3 Schematic view of an etch pit for the charged particle having certain incident angle.

### III. Results and Discussions

#### 1. Alpha particle mapping on cellular image

Figure 4 is typical image of alpha/lithium tracks and transmission X-ray image of tumor cells as relief observed simultaneously on a CR-39 plate with an AFM. Height information is represented such that brighter region corresponds to higher region, and darker to lower. We can see cell nucleus as round shaped object of relief in the image as similarly shown

in transmission electron microscopy. Alpha/lithium tracks are also visualized as etch pits in the image.

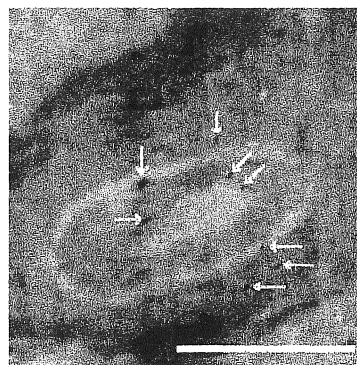


Fig. 4 Typical image of alpha/lithium tracks and transmission X-ray image of a tumor cell as relief on a CR-39 plate observed with an AFM. Arrows indicates alpha/lithium tracks. Scale bar corresponds to  $5 \mu\text{m}$ .

#### 2. Discrimination between alpha/lithium particles and proton background

Figure 5 shows the relations between the radius of small etch pits and LET of irradiated protons or alpha particles. The diameter tends to increase systematically as LET value becomes larger even for small etch pits of several tens of nanometers in radius. The average critical angles were derived from the track sensitivity of the etch pits for those particles. Those were  $47^\circ$  for alpha/lithium particles, and  $25^\circ$  for protons respectively (the amount of bulk etch was about  $150 \text{ nm}$  in the present experiments). In the condition of the present experiments, the maximum travel length of alpha/lithium particles through the biological specimen ( $1 \mu\text{m}$ -thick) having the incident angle near the critical angle ( $47^\circ$ ), is about  $1.4 \mu\text{m}$ . This means that when the alpha/lithium particles impact CR-39 surface, the energies for those particles with maximum travel length are about  $1 \text{ MeV}$  ( $\sim 220 \text{ keV}/\mu\text{m}$  in LET) for alpha particles and about  $300 \text{ keV}$  ( $\sim 200 \text{ keV}/\mu\text{m}$ ) for lithium respectively. Therefore, eliminating the counts for the particles having the LET value of less than  $100 \text{ keV}/\mu\text{m}$  will enable us to discriminate only alpha/lithium particles from background protons.

The size distribution of the etch pits for the experiment of discrimination between alpha particles and protons are shown in Fig. 6. In Fig. 6, the size spectrum of proton etch pits only is also presented. Around 9 pixels ( $= 68 \text{ nm}$  in diameter), we can discriminate alpha particles from protons. The number of each particle discriminated with the size threshold was confirmed to be same as that of each irradiated particles.

#### 3. Incident angle measurement

Figure 7 shows the results of the incident angle measurements. Near the normal incident ( $= 90^\circ$ ), the measured incident angle with only mouth shape of the etch pits were much underestimated, on the other hand, the results with three di-

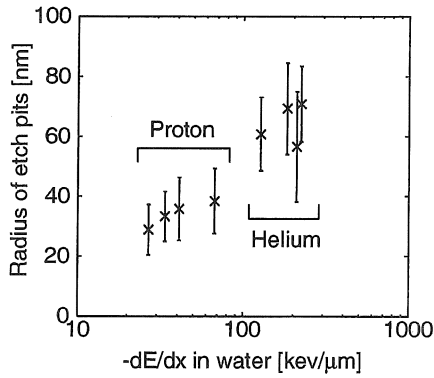


Fig. 5 Relation between LET and size of etch pits for incident charged particles.

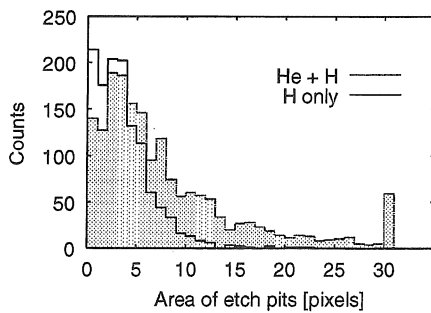


Fig. 6 Histogram for the size of etch pits in the present experiment. See text for the details.

dimensional shape of the etch pits show good agreement with the nominal incident angle. Although the accuracy of the measurements was several degrees, the uncertainty of positioning incident charged particle will be within 200 nm since the thickness of the sample we use in NIAR for BNCT is about 1  $\mu\text{m}$ . It is sufficient for the subcellular charged particle mapping.

#### IV. Conclusion

We have demonstrated subcellular alpha-track mapping on cellular image using CR-39 plastics and an AFM with contact X-ray microscopy technique. We have also examined the relation between the size of etch pits and LET of charged particles, and the measurement of incident angle of charged particles by the shape of etch pits on CR-39 plastics with AFM readout.

Alpha particles with the energy of MeV order, which are main component in the NIAR, and protons can be discriminated by the size of etch pits even with AFM observation since those alpha particles have larger LET value than protons. Therefore the background protons can be eliminated in the high-resolution NIRA.

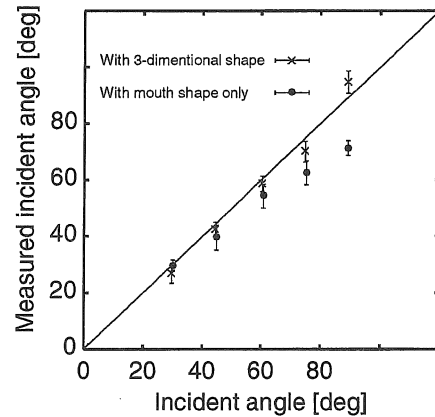


Fig. 7 Results of incident angle measurement in the present experiments. See text for the details.

Using three-dimensional shape of etch pits, measured with an AFM, the incident angle of charged particles can be derived more accurately than only from the mouth shape of those etch pits. The uncertainty was about several degrees.

Those experiments approved the reliability of the high-resolution NIRA for the measurements of boron compound distribution inside a cell at subcellular scale in BNCT.

#### Acknowledgements

The authors thank the staff members of RCNST, The University of Tokyo, KUR and NIRS-HIMAC for their support during the experiments. A part of this research was supported by Research Fellowship of the Japan Society of the Promotion of Science (JSPS) for Young Scientists and Grant-in-Aid for Scientific Research of JSPS. A part of this research was also supported by the research fund from Association for Nuclear Technology in Medicine, Japan.

#### References

- 1) G. R. Solares and R. G. Zamenhof, *Radiat. Res.*, **144**, 50 (1995).
- 2) H. Yanagie, et al., *Nucl. Inst. Meth.*, **B424**, 122 (1999).
- 3) H. Hatanaka and Y. Nakagawa, *Int. J. Radiat. Oncol. Biol. Phys.*, **28**, 1061 (1994).
- 4) K. Amemiya, et al., *Nucl. Inst. Meth.*, **B159**, 75 (1999).
- 5) T. Tomie, et al., *Science*, **252**, 691 (1991).
- 6) H. Shimizu, et al., In: *X-ray microscopy and spectromicroscopy*. Heidelberg: Springer-Verlag; 1996. p.I-157 (1996).
- 7) K. Amemiya, et al., *Nucl. Inst. Meth.*, **B187**, 361 (2002).
- 8) J. Skvarč, et al., *Nucl. Inst. Meth.*, **B152**, 115 (1999).
- 9) K. Yoshida, et al., *Ionizing Radiation*, **23**, 113 (1997) [in Japanese].